RESISTIVITY AND 'm' VARIATION WITH PRESSURE*

Lloyd N.S. Kunar
Department of Chemical Engineering
University of the West Indies
St. Augustine
Republic of Trinidad & Tobago

Summary

Resistivity measurements at various differential pressures are made on hard sandstone core samples saturated with sea water. The results are explained in terms of the distribution of cracks and pores and their closure dependence on pressure. The pore spectrum distribution is determined from seismic velocity measurements.

The "cementation factor", m, is computed from $F = 1/C^m$, where C is the porosity. Three distinct regions, in each of which m is evaluated as a linear function of depth, seem evident. The study of m versus porosity/differential pressure is unique in that a single sample is sufficient to do so.

INTRODUCTION

The resistivity of a rock depends on the resistivity of its matrix and the usually lower resistivity of the fluid filling the pores and cracks. It is therefore obvious that the measured resistivity of a specific rock type is determined primarily by its fluid content or porosity.

Generally, all rocks possess pores and cracks of various sizes and shapes which can be characterized by an aspect ratio and concentration distribution. The aspect ratio is equivalent to the ratio of the minor to the major axis of a spheroidal cavity. As pressure increases, the finer pores and cracks close thereby modifying the porosity as well as the elastic moduli and density. These modifications produce changes in resistivity and seismic velocity which are usually substantial during the initial stages of incremental pressure increases. At higher pressures the cracks become closed and the spherical pores undergo such small changes in volume with further increases in pressure that both the resistivity and seismic velocity changes at these pressures are minimal.

As is to be expected, the total pore volume depends on the fluid pressure, P_f, within it, and on the confining pressure, P_c, of the overburden. The difference, $(P_c - P_f)$, between these pressures gives the grain or differential pressure, P_d, determining the pore volume. At a differential pressure of 200 bars ($\sim$ 1615 m), cracks with aspect ratios (α) less than 10^{-4} are closed while those with α in the range 10^{-2} to 10^{-4} become thinner. At a P_d of 500 bars ($\sim$ 4020 m), all pores with α less than 10^{-2} are closed. At higher pressures the spherical pores decrease in volume but not in shape.

In this study, the resistivity is measured as a function of differential pressure and the porosity is computed from corresponding measurements of the compressional wave velocity. The theories of Kuster and Toksoz (1974) and Toksoz et al (1976) enable the computations.

The resistivity of a compacted sandstone sample is analyzed. The applicable relationship for the formation factor F is assumed to be of the form:

$$F = \frac{1}{C^m} \qquad \ldots\ldots (1)$$

*paper presented at the Society of Petroleum Engineers Exposition and Conference held in March 1980 at Port-of-Spain, Trinidad.

where C is the total porosity. Equation (1) in conjunction with,

$$F = \frac{R_o}{R_w} \qquad \ldots\ldots (2)$$

enables m, the cementation factor, to be evaluated at various differential pressures or depths. R_o is the resistivity of the sample 100% saturated with sea water of resistivity R_W.

The technique for determining m at various pressures is unique in that it requires a single sample and not many as has been required by other workers.

EXPERIMENTAL PROCEDURE AND RESULTS

Cylindrical specimens ($\sim$25 mm diam. x $\sim$ 25 mm length) were cut from hard sandstone cores obtained from a depth of 3050m in an oil producing area. These were cleaned with toluene and over-dried for seismic velocity and resistivity measurements. The saturant used was sea water of resistivity (R_W) 0.04 ohm-m. The elastic parameters for the matrix and fluid were both known.

The apparatus for measuring seismic velocity was identical to the one described by Wyllie et al (1958). Their paper provides a detailed diagram of the velocity differential pressure cell. The cell together with a standard Wheatstone bridge circuit was used to determine conductivity.

During the experiments, the saturant was kept at atmospheric pressure so that its properties remained constant. The matrix or overburden pressure was varied to produce the pressure differential, P_d. Since matrix properties do not change significantly with pressures up to 1 kilobar or more, there was no need to alter these in the calculations.

Figures 1 and 2 show the results for two samples A2 and B2. B2 shows appreciable hysteresis in seismic velocity due to inelastic deformation. It was therefore not used to exemplify the behaviour of resistivity with pressure. Sample A2, on account of its elastic behaviour, constitutes the example discussed in this paper. It is seen that the velocity increase and the conductivity decrease are rapid at low pressures (0-0.2 Kb or 0-1830 m) and much slower for greater pressures. Qualitatively this seems to be in accord with the reactions of cracks and pores under increasing differential pressure.

In order to relate the resistivity values to the cementation factor, m, the total porosity, C, must be evaluated at each pressure.

POROSITY DETERMINATION

Measurements of compressional wave velocities at various pressure differentials are used to compute the porosity. The "time average" equation proposed by Wyllie et al (1956) is not employed, because of the dubious assumption on which it is based. That is, a saturated porous medium can be treated as a series of alternating solid and liquid layers with the wavefront traversing the interfaces in a perpendicular direction. Wyllie's equation is sufficiently accurate at high differential pressures but inadequate at low pressures when the microcracks are open.

The method of Kuster and Toksoz (1974) based on scattering theory, is used to obtain the porosities. Essentially, they obtained composition laws for effective elastic constants and densities of materials containing both spherical and spheroidal inclusions. These parameters enable the computation of compressional velocities which are then compared with the experimental values for closeness of fit.

In any rock, there is usually a mixture of pore sizes ranging from spheres to thin cracks each of which is characterised by an aspect ratio α_m (ratio of minor to major axis). If $C(\alpha_m)$ represents the concentration of pores having an aspect ratio α_m, then,

$$\frac{K^* - K}{3K^* + 4\mu} = \frac{1}{3}\,\frac{K' - K}{3K + 4\mu} \sum_{M=1}^{M} c(\alpha_m) \cdot T_{iijj}(\alpha_m) \qquad \ldots\ldots (3)$$

$$\frac{\mu^* - \mu}{6\mu^*(K+2\mu) + \mu(9K+8\mu)} = \frac{\mu' - \mu}{25\mu(3K+4\mu)} \sum_{M=1}^{M} c(\alpha_m) \cdot \left[T_{ijij}(\alpha_m) - \frac{1}{3} T_{iijj}(\alpha_m) \right] \qquad \ldots\ldots\ (4)$$

and

$$c = \sum_{M=1}^{M} c(\alpha_m) \qquad \ldots\ldots\ (5)$$

C represents the total concentration of inclusions, or simply the total porosity. The quantities (K, μ, ρ) refer to the bulk modulus, rigidity modulus, and density of the matrix, the primed quantities (K', μ', ρ') to the inclusions, and the starred quantities (K^*, μ^*, ρ^*) to the effective properties of the composite. Once the starred quantities are obtained, the compressional or P-wave velocity is calculated using:

$$V_p = \sqrt{K^*/\rho^*} \qquad \ldots\ldots\ (6)$$

T_{iijj} and T_{ijij} are scalars which are functions of the shapes of the pores and cracks. The procedure for calculating these quantities for each aspect ratio, α, is as follows:

$$T_{iijj} = + \frac{3F_1}{F_2}$$

$$T_{ijij} - \frac{1}{3} T_{iijj} = \frac{2}{F_3} + \frac{1}{F_4} + \frac{F_4F_5 + F_6F_7 - F_8F_9}{F_2F_4}$$

$$F_1 = 1 + A \left[\frac{3}{2}(g+\phi) - R \left\{ \frac{3}{2} g + \frac{5}{2} \phi - \frac{4}{3} \right\} \right] \qquad \ldots\ldots\ (7)$$

$$F_2 = 1 + A \left[1 + \frac{3}{2}(g+\phi) - \frac{R}{2}(3g+5\phi) \right] + B(3-4R) + \frac{A}{2}(A+3B)(3-4R) \left[g+\phi - R(g-\phi+2\phi^2) \right]$$

$$F_3 = 1 + \frac{A}{2} \left[R(2-\phi) + \frac{(1+\alpha^2)}{\alpha^2} g(R-1) \right],$$

$$F_4 = 1 + \frac{A}{4} \left[3\phi+g-R(g-\phi) \right],$$

$$F_5 = A\left[R\left\{g+\phi-\frac{4}{3}\right\} - g\right] + B\phi(3-4R),$$

$$F_6 = 1 + A\left[1+g-R(g+\phi)\right] + B(1-\phi)\ (3-4R) \qquad \ldots\ldots (7)$$

$$F_7 = 2 + \frac{A}{4}\left[9\phi+3g-R(5\phi+3g)\right] + B\phi(3-4R),$$

$$F_8 = A\left[1 - 2R+\frac{g}{2}(R-1) + \frac{\phi}{2}(5R-3)\right] + B(1-\phi)\ (3-4R),$$

$$F_9 = A\left[g(R-1) - R\phi\right] + B\phi(3-4R).$$

$$A = \frac{\mu'}{\mu} - 1, \quad B = \frac{1}{3}\left\{\frac{K'}{K} - \frac{\mu'}{\mu}\right\}, \quad R = \frac{3\mu}{3K + 4\mu},$$

$$\phi = \frac{\alpha}{(1-\alpha^2)^{3/2}}\left[\mathrm{Cos}^{-1}\alpha - \alpha(1-\alpha^2)^{\frac{1}{2}}\right], \quad g = \frac{\alpha^2}{1-\alpha^2}(3\phi - 2).$$

To determine V_p, the pore distribution, $C(\alpha_m)$, in the sample must be stipulated at each differential or grain pressure. Actually it is only necessary to do so at one pressure, usually atmospheric pressure, when the fine cracks $(\alpha < 10^{-3})$ are open. Other pore distributions can then be ontained using the approaches of Toksoz et al (1976) and Kuster and Toksoz (1974).

The pore distribution at atmospheric pressure is determined by measuring the seismic velocity, V_p, at that pressure and then assuming various spectra until the theoretical V_p matches the experimental value. Often scanning electron microscope (SEM) photographs are used, as in this study, to make the initial assumption of the pore spectrum. The uniqueness of the theoretical spectrum has been discussed by Cheng and Toksoz (1978), who showed that concentrations of pores with aspect ratios greater than about $\alpha = 10^{-4}$ can be determined uniquely.

For an applied pressure differential of P_d, the dilation of the applied strain field is:

$$\varepsilon = \frac{-P_d}{K^*_A}$$

where K^*_A is the effective static bulk modulus. It is computed from:

$$K_A^* = \left[\frac{K - \dfrac{4\mu c K}{3(3K + 4\mu)} T_{iijj}}{1 + \dfrac{cK}{(3K + 4\mu)} T_{iijj}} \right] \qquad \text{..... (9)}$$

ε is defined as:

$$\varepsilon = \frac{-dc}{c} \qquad \text{....... (10)}$$

where c is the pore volume and dc the incremental charge due to the applied stress.

Using equations (8) and (10) and the expressions for the strain field (Eshelby, 1957) just outside an ellipsoidal cavity, Toksöz et al (1976) showed that:

$$\frac{dc}{c} = - \frac{P_d}{K_A^*} \Big/ \left[E_1 - E_2/E_3/(E_3 + E_4) \right], \qquad \text{....... (11)}$$

where,

$$E_1 = \frac{6\mu I}{2\pi(3K+4\mu)}$$

$$E_2 = \frac{6\mu}{4\pi(3K+4\mu)} \quad (3I-4\mu)$$

$$E_3 = \frac{\alpha^2(3-9I/4\mu)(6K+2\mu)}{2(1-\alpha^2)(3K+4\mu)} + \frac{6\mu I}{8\pi(3K+4\mu)}$$

$$E_4 = \frac{1}{2} \left[\frac{(3-9I/4\mu)\ \ (6K+2\mu)}{2(1-\alpha^2)\ \ (3K+4\mu)} - \frac{3\mu(I-I/\pi)}{3K+4\mu} \right]$$

and,

$$I = \frac{2\pi\alpha}{(1-\alpha^2)^{3/2}} \left[\cos^{-1} \alpha - \alpha(1-\alpha^2)^{\frac{1}{2}} \right] \qquad \text{..... (12)}$$

Thus for any aspect ratio, α_m, the corresponding dc_m can be found and hence the change, dc, in total pore volume:

$$dc = \Sigma dc_m \qquad \text{...... (13)}$$

The new pore volume at the particular pressure, P_d, is therefore (c — dc).

In this study, the P-wave velocities are found at differential pressures up to 1 kilobar, corresponding to a depth of approximately 7925 m, figure 1. The pore spectrum distribution is then established so that the theoretical and experimental values of V_p are in satisfactory agreement. Knowing the spectrum at atmospheric pressure, the porosity for every differential pressure is calculated. The conductivity—P_d, plot of figure 2 is then easily transformed to the resistivity-porosity plot of figure 3.

DISCUSSION OF RESULTS

The resistivity-porosity plot for sample A2 (figure 3) exhibits a trend similar to the resistivity-differential pressure plot — figure 2. The resistivity increases markedly as the porosity drops from 14 percent to 10 percent. Thereafter the increase is not as pronounced.

Table 1 summarises the results of this study. The formation factor, F, is calculated using equation (2) and subsequently m is determined using equation (1). It is therefore possible to study the behaviour of m with pressure or depth of burial — figure 4.

The "cementation factor" seems to display three trends corresponding to shallow (0-305 m), moderate (305-1830 m), and greater (1830-9150 m) depths. For the shallow depths, m increases most rapidly from 2.00 to 2.33; for the moderate depths, m decreases at a slow rate from about 2.33 to 2.12; and for greater depths, m decreases at an even slower rate from 2.12 to about 1.90. If D represents the depth in kilometres to a particular point, then the behaviour of m can be satisfactorily represented by three linear equations:

SHALLOW DEPTHS: $m = 2.00 + 0.994D$ .... (14)

MODERATE DEPTHS: $m = 2.40 - 0.151D$ .... (15)

GREATER DEPTHS: $m = 2.12 - 0.026D$ .... (16)

CONCLUSION

Generally, for reservoirs normally pressured and in the depth range 2500-6000 m, m ranges between 2.10 and 2.00 values which are in close agreement with the much used value of m = 2.00. This value of m has been used so often that it is accepted and applied without reservation to all depths and to both under and over-pressured regions. The latter determines the differential pressure and therefore the value of m to be used in any accurate determination of porosity.

As was mentioned before, this method of determining m, is unique in that only a single sample is required. It should therefore be quite feasible to determine m for an environment in which porosity variations are small and for which only few core samples exist.

The resistivity behaviour with pressure seems to be in accord with predictions of the theories of cracks and pores.

TABLE 1

C%	P_d KB	$F = R_o/R_w$	m in $F = \frac{1}{C^m}$	Equivalent Depth ft	m	P_d psia
14.0	0	50.5	2.0	0	0	0
13.5	0.02	75.0	2.16	527	160	290
13.0	0.025	97.5	2.24	659	200	363
12.0	0.04	137.5	2.32	1054	320	580
11.0	0.06	170.0	2.33	1582	480	870
10.2	0.075	185.0	2.29	1977	600	1088
9.4	0.15	201.5	2.24	3954	1205	2175
8.2	0.225	208.25	2.13	5931	1808	3263
7.8	0.3	211.75	2.10	7908	2410	4350
7.4	0.45	214.5	2.06	11862	3615	6525
7.2	0.60	217.5	2.05	15816	4820	8700
6.8	0.75	219.25	2.01	19770	6025	10875
6.5	0.90	220.25	1.97	23724	7230	13050
6.4	1.05	220.75	1.96	27678	8436	15225

REFERENCES

1. CHENG, C.H., and TOKSOZ, M.N., "Pore and Crack Aspect Ratio Spectrum Determination from Seismic Velocity Data". 1976, EOS, V. 57, p. 324.
2. ESHELBY, J.D., "The Determination of the Elastic Field of an Ellipsoidal Inclusion, and Related Problems". 1957, Proc. Roy. Soc. London, ser. A. V. 241, pp. 376-396.
3. KUSTER, G.T., and TOKSOZ, M.N., "Velocity and Attenuation of Seismic Waves in Two-Phase Media": 1974, Part I — Theoretical Formulations, Geophysics, V. 39, pp. 587-606; Part II — Experimental results. Geophysics, V. 39, pp. 607-618.
4. TOKSÖZ, M.N., CHENG, C.H., and TIMUR, A. "Velocities of Seismic Waves in Porous Rocks". 1976, Geophysics, V. 41, pp. 621-645.
5. WYLLIE, M.R.J., GREGORY, A.R., and GARDNER, G.H.F. "An Experimental Investigation of Factors Affecting Elastic Wave Velocities in Porous Media". 1958, Geophysics, V. 23, pp. 459-493.

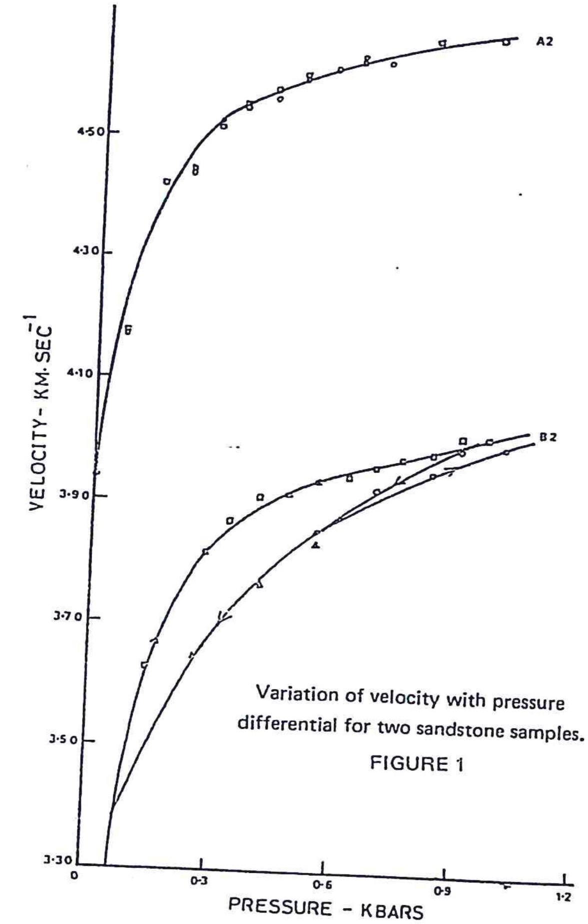

Variation of velocity with pressure differential for two sandstone samples.
FIGURE 1

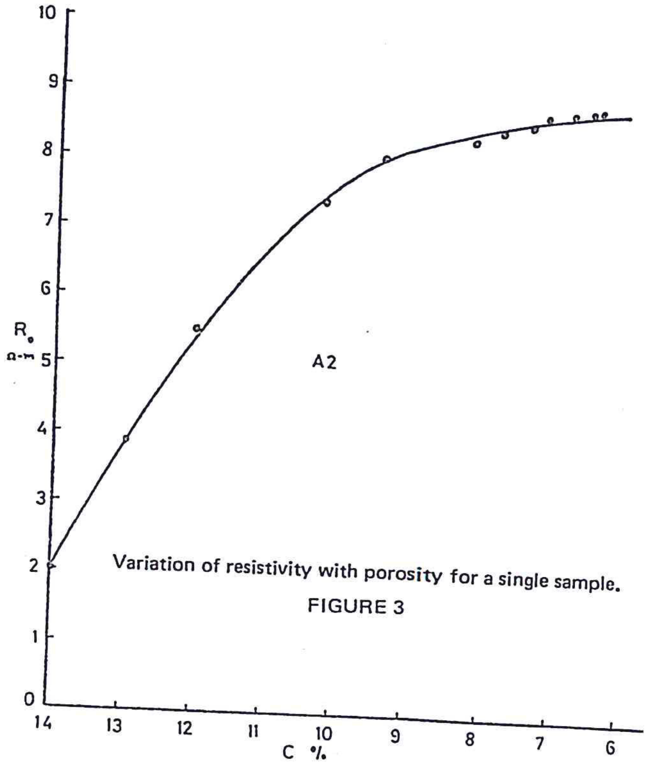

Variation of resistivity with porosity for a single sample.
FIGURE 3

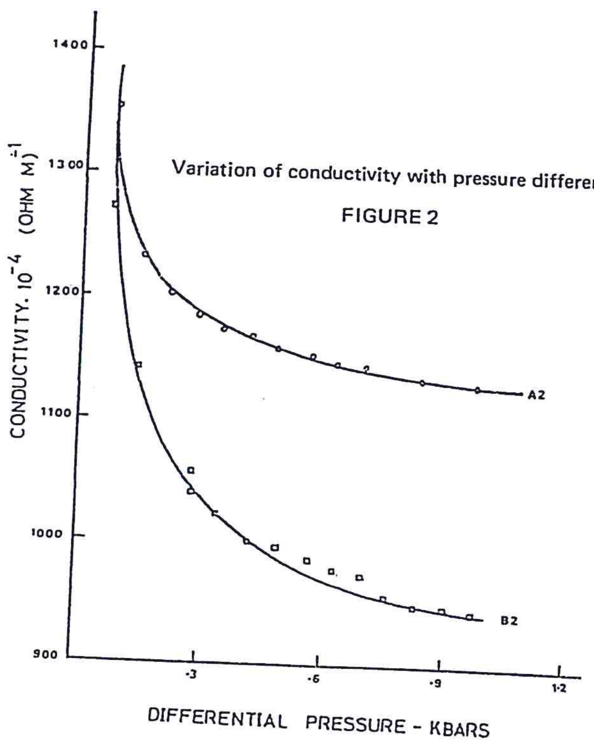

Variation of conductivity with pressure differential.
FIGURE 2

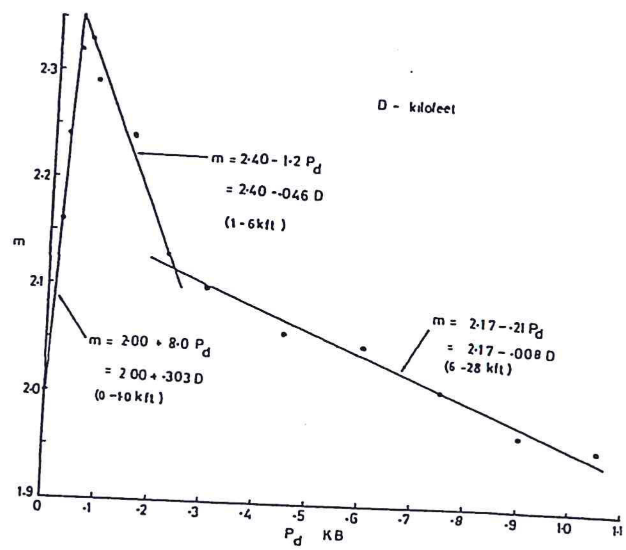

M-Variation with depth.
FIGURE 4